Proton-Assisted Electron Transfer in Irradiated DNA−Acrylamide Complexes: Modeled by Theory

Jessica Taylor, Isaac Eliezer, and Michael D. Sevilla*

Chemistry Department, Oakland University, Rochester, Michigan 48309

Received: July 26, 2000; In Final Form: November 27, 2000

Theoretical calculations at the density functional theory (DFT) level are employed to elucidate a proton-assisted electron transfer (PA-ET) reaction within a DNA base (thymine)−acrylamide hydrogen-bonded complex, a process suggested from previous experimental results. Calculations with a 6-31+G* basis set are performed with full geometry optimizations and with vibrational analysis. Theory predicts the initial unpaired spin is delocalized over both thymine and acrylamide, and proton transfer then serves to fully localize the spin to the acrylamide. The PA-ET reaction is found to be exergonic by 1.6 kcal/mol. The final step of the reaction, i.e., an intramolecular proton transfer from the oxygen to the terminal carbon on acrylamide, results in the experimentally observed radical, i.e., $CH_3CH(\bullet)CONH_2$, and is also predicted to be highly exergonic (18 kcal/mol).

Introduction

Proton-assisted electron transfer (PA-ET) mechanisms were initially proposed in the 1960s[1,2] with little experimental evidence to support them. At present they are accepted as important to many biological processes.[3] These include charge-transfer stabilization, multielectron substrate oxidation,[4,5] photoinduced electron transfer,[6,7] proton gradient generation,[1b,8,9] and rates of electron transfer.[9−12] However, such mechanisms have been reported in only a few DNA-related systems.[13,14] PA-ET mechanisms are pertinent to radiation damage processes in DNA and are very likely a fundamental controlling mechanism in electron transfer within DNA. It is now realized that reversible proton transfers stabilize charged DNA intermediates in deeper potential wells and thereby inhibit electron/hole transfer processes.[12] The reverse proton transfer then proceeds before continued electron transfer through the strand; as a consequence, proton transfer between base pairs slows electron transfer in DNA.[12]

We have chosen to theoretically investigate an example of PA-ET in the acrylamide−DNA complex because of previous experimental results that suggested such a process.[15] Acrylamide is an electron-affinic compound that is also able to hydrogen bond to DNA bases. It is well-known that acrylamide is an efficient electron scavenger in frozen aqueous glasses.[16] Experimental results show that the acrylamide anion radical formed by electron attachment to the acrylamide is accompanied by protonation at the terminal carbon atom even at 77 K[16] according to reaction 1.

$$CH_2{=}CHCONH_2 + e^- \rightarrow CH_2{=}CHC(\bullet)O^-NH_2 \xrightarrow{H^+} CH_3CH(\bullet)CONH_2 \quad (1)$$

It is also known[17] that similar amides form complexes with DNA via hydrogen bonding to thymine with the displacement of adenine. ESR studies of hydrated DNA samples show that activated electron transfer through DNA is not found below 160 K.[18−20] However, experimental results show that while acrylamide when bound to DNA scavenges electrons poorly at 77 K, it appears to scavenge well at 130 K; i.e., electron transfer from DNA to acrylamide occurs on thermal annealing of irradiated DNA−acrylamide complexes to 130 K.[15] In fact, the neutral radical species formed after electron attachment to acrylamide can be used to measure the variation of local DNA electron transport processes with temperature.[15]

The thermally induced transfer of electrons from the electron gain centers of DNA to the acrylamide is surprising and points to an intermediate process. The reaction scheme depicted in reactions 2−4 indicates that hydrogen bonding to DNA (via the amide functional group) provides sufficient electronic coupling for electron transfer to the acrylamide to occur to the final reaction by protonation of the anion radical. But this scheme does not explain the reasons for the initial stabilization on DNA and the subsequent transfer to acrylamide. Presumably if the thymine or cytosine base were more electron affinic at 77 K, it would remain so at 130 K.

$$DNA{:}CH_2{=}CHCONH_2 + e^- \rightarrow DNA^-{:}CH_2{=}CHCONH_2 \quad 77\ K \quad (2)$$

$$DNA^-{:}CH_2{=}CHCONH_2 \xrightarrow{ET} DNA{:}CH_2{=}CHC(\bullet)O^-NH_2 \quad 130\ K \quad (3)$$

$$DNA{:}CH_2{=}CHC(\bullet)O^-NH_2 \xrightarrow{PT} DNA[-H^+]^-{:}CH_3CH(\bullet)CONH_2 \quad 130\ K \quad (4)$$

The explanation for the electron transfer which we propose is that proton transfer from a DNA base (e.g. thymine) to acrylamide assists an electron transfer from the DNA base to acrylamide (Figure 1, reaction A*)*. This proposal is tested in the present work by means of a density functional approach. Employing a thymine−acrylamide model system, DFT calculations are found to substantiate the proposed mechanism. A similar mechanism has been proposed recently for long-range electron transfer in redox enzymes.[21−22]

10.1021/jp0026540 CCC: $20.00
Published on Web 01/25/2001

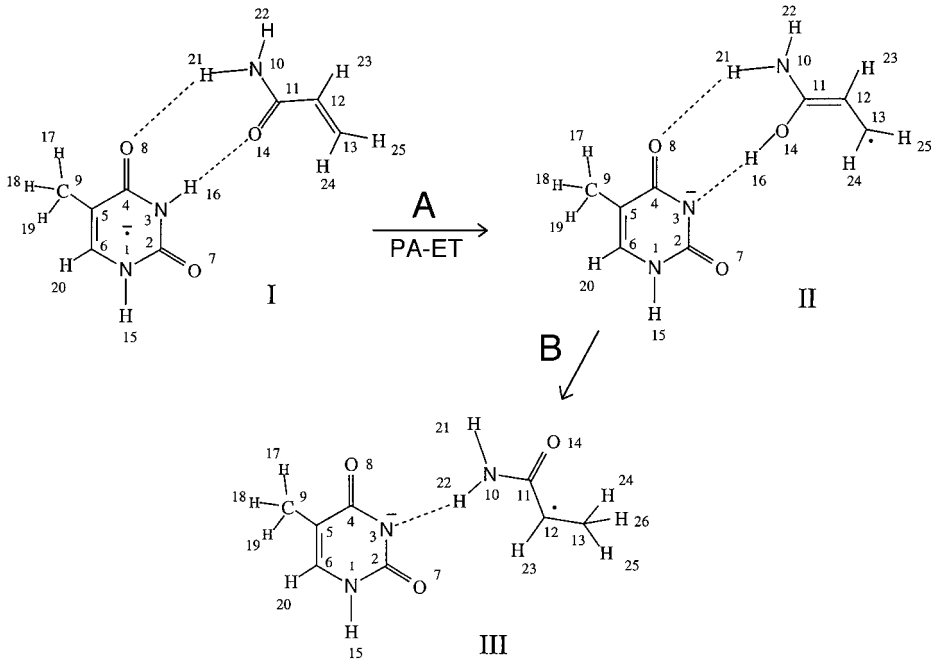

Figure 1. Reactions for the thymine−acrylamide complex after electron capture showing the PA-ET step (reaction A) and the rearrangement to the final product, **III** (reaction B). The numbering of all atoms is also shown. Species **I** is the thymine−acrylamide complex with the electron on the thymine or shared with acrylamide. Species **II** is the complex with the electron fully on acrylamide stabilized by proton transfer from thymine to the acrylamide. Species **III** is the complex after rearrangement.

Methods and Calculations

In this work we model the DNA−acrylamide complex through the use of the simpler thymine−acrylamide hydrogen-bonded complex. Molecular orbital calculations have been performed with density functional theory (DFT) at the B3LYP level. As recently pointed out, DFT calculations give excellent predictions of electron affinities, molecular geometry, and thermodynamic properties.[23,24]

The Gaussian 98 program was employed for all DFT calculations in this study.[25] The Spartan program, from Wavefunction, Inc., was used for the graphical models shown in this work. All DFT calculations were carried out with the 6-31+G* polarization basis set for isolated molecules. Full geometry optimizations were performed for all structures presented in this work. Full vibrational calculations were also performed to obtain zero point vibrational energies and thermal corrections to 298 K. In this manner, gas phase energies, enthalpies, free energies, and entropies were computed for the species shown in Figure 1. The influence of the surroundings cannot be accurately modeled since unknown details of base stacking and specific hydration waters would need to be included. However, in previous work these effects were suggested to be energetically small for proton transfer between hydrogen-bonded DNA bases.[12c,d] This is in part due to the fact that the dielectric constant in the DNA base stack is low (ca. 2).[12c]

Spin densities, hyperfine couplings, and charge densities were also calculated. The calculated results for DFT energies are given in Table 1. In the table calculated values for the Hartree Fock energies (E_{HF}), zero point vibrational energy corrected Hartree Fock values (E_o), the thermodynamically corrected energy at 298 K (E_{298}), the enthalpy at 298 K (H_{298}), the entropy at 298 K (S_{298}), and the free energy at 298 K (G_{298}) are all reported. Table 2 reports differences in the enthalpies, free energies, and entropies reported in Table 1, appropriate for the various reactions described in this work. Note that for an intermolecular proton-transfer reaction in isolated molecules, there is no significant PV energy difference between products and reactants, so that little difference between enthalpies and energies of reaction is found. The results for the calculations of spin densities and charge densities are given in Table 3 for species **I** and **II**.

TABLE 1: DFT Calculated Energies (in au) and Entropies (in cal/(mol K))[a]

energy	species **I**	species **II**	species **III**
E_{HF}	−701.490 378	−701.494 721	−701.517 905
E_o	−701.300 232	−701.303 413	−701.326 876
E_{298}	−701.284 727	−701.288 463	−701.311 223
H_{298}	−701.283 783	−701.287 519	−701.310 279
G_{298}	−701.345 149	−701.347 710	−701.374 002
S_{298}	129.15	126.68	134.05

[a] E_{HF} is the Hartree−Fock energy with the 6-31+G* basis set. E_0 includes the zero point vibrational energy. E_{298}, H_{298}, G_{298}, and S_{298} are the respective thermodynamic values including thermodynamic corrections up to 298 K.

TABLE 2: DFT Reaction Enthalpies, Entropies, and Free Energies[a]

reacn/species	ΔH, kcal/mol	ΔS, cal/(mol K)	ΔG, kcal/mol
(A) **I** → **II**	−2.3	−2.5	−1.6
(B) **II** → **III**	−14.3	7.4	−18.1
(overall) **I** → **III**	−16.6	4.9	−19.7

[a] Calculated from the data in Table 1.

Discussion

We have performed theoretical calculations at the DFT level for structures of the radical anion of DNA−acrylamide before and after PA-ET (Figure 1, reaction A). In addition we have modeled the subsequent rearrangement to the final radical observed experimentally (Figure 1, reaction B). The DFT energies, enthalpies, and entropies are given in Table 1, while in Table 2 we summarize the overall thermodynamic energy changes for the reactions. Clearly both reactions A and B are exothermic and exergonic. Thus DFT calculation predicts the PA-ET (reaction A) to be favorable with an equilibrium constant

TABLE 3: DFT Spin Densities and Charge Densities for Species I and II

		species **I**		species **II**	
posn	atom type	spin density	charge density	spin density	charge density
1	N	0.0254	−0.6344	0.0000	−0.5854
2	C	−0.0027	0.7305	−0.0006	0.6245
3	N	0.0360	−0.7380	0.0003	−0.7215
4	C	0.1449	0.5313	0.0011	0.5156
5	C	−0.0167	0.0645	−0.0069	0.7510
6	C	0.3695	−0.0406	0.0013	−0.6171
7	O	−0.0005	−0.5631	−0.0001	−0.5949
8	O	0.0656	−0.6171	0.0000	−0.6220
9	C	−0.0013	−0.4992	−0.0000	−0.8848
10	N	0.0154	−0.8015	0.0778	−0.8477
11	C	0.0928	0.5277	0.3271	0.2651
12	C	0.0192	−0.1403	−0.1150	0.0799
13	C	0.2749	−0.3702	0.7342	−0.7295
14	O	0.0393	−0.5818	0.0493	−0.6704
15	H	−0.0026	0.3063	−0.0000	0.4170
16	H	−0.0019	0.3971	−0.0016	0.5719
17	H	−0.0011	0.1400	−0.0000	0.2191
18	H	−0.0009	0.1389	−0.0000	0.2184
19	H	−0.0004	0.0102	0.0000	0.1688
20	H	−0.0223	0.0945	−0.0000	0.1650
21	H	−0.0002	0.3872	0.0022	0.4859
22	H	−0.0005	0.2811	−0.0027	0.3481
23	H	−0.0028	0.0645	0.0005	0.1202
24	H	−0.0143	0.1381	−0.0327	0.1839
25	H	−0.0150	0.2817	−0.0343	0.1384

at room temperature of about 15. However, the second reaction is predicted to be highly exergonic and would drive the reaction to the final product (Figure 1, species **III**).

Entropic effects are small and negative in the first reaction but are larger in magnitude and positive in the second as a result of the formation of the methyl group and the breaking of a hydrogen bond. It is clear that a consideration of the surroundings would also produce entropic effects comparable to those calculated for the isolated molecules. However, the energy change is large and will dominate the overall process.[12c,d]

The fact that the electron is shared in the DFT calculation suggests nearly equal EA for the components of the complex before PA-ET. This is verified by a calculation of the LUMO energies of thymine and acrylamide. DFT predicts that the thymine LUMO is only 0.16 eV more stable than that of acrylamide.

The spin and charge density results given in Table 3 are summarized in graphic form in Figure 2. In Figure 2 we see that the predicted spin density on species **I**, depicted by light gray regions, is shared over both the thymine and acrylamide. However, on proton transfer from N3 on thymine to the oxygen on acrylamide forming species **II**, the electron spin distribution changes dramatically as shown in Figure 2B. As can be seen the unpaired spin density shifts fully to acrylamide. Figure 1 gives the numbering of all the atoms in the complexes and so allows a comparison of the numerical values in Table 3 for key atoms in species **I** and species **II**. This points to the same conclusions as Figure 2.

Reaction B (Figure 1) shows the intramolecular and likely irreversible proton transfer reaction from the oxygen on acrylamide to the carbon to form species **III**, i.e., the final product observed by experiment. The rearrangement from **II** to **III** (after the proton transfer) involves an altering of the hydrogen bonding between thymine and acrylamide by rotation and translation of the acrylamide so that the hydrogen bond moves from the oxygen to the negatively charged nitrogen. These later processes are less energetically driven than the intramolecular proton

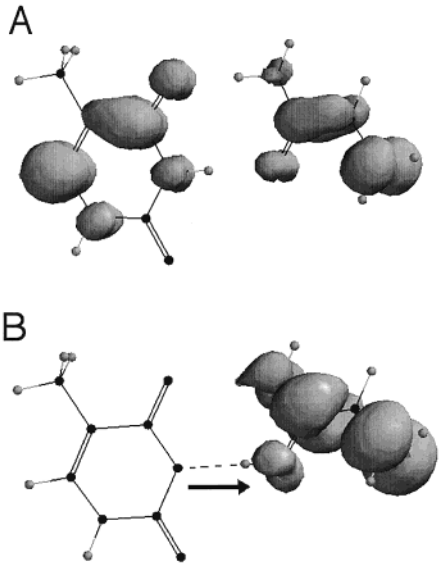

Figure 2. Spin density distributions for thymine−acrylamide complexes after electron capture. (A) DFT spatial spin distribution for species **I** (before PA-ET). Note that the spin is shared over both the thymine and acrylamide structures at the 0.002 spin contour. (B) DFT spatial spin distribution for species **II** (after PA-ET) at the 0.002 spin contour.

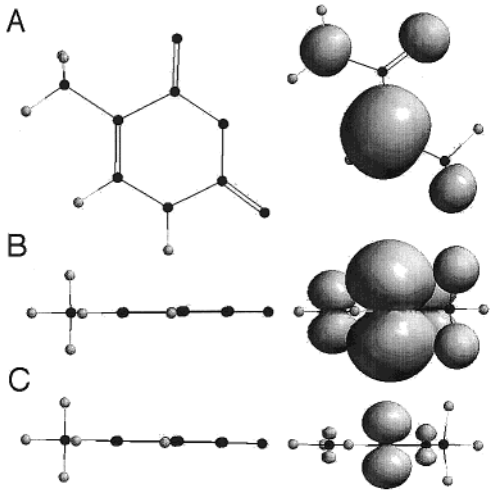

Figure 3. Spin density distribution for radical **III**. This radical is formed by electron attachment to the thymine−acrylamide complex followed by PA-ET and rearrangement. (A) DFT spatial spin distribution at 0.002 density contour. (B) Edge view DFT spatial spin distribution in (A). (C) Edge view DFT spatial spin distribution in (A) at 0.02 density contour.

transfer but add to the stabilization of the product. Radical **III** has its spin density largely localized to the α-carbon of the acrylamide (C-12). Figure 3 A,B shows the face and edge views of the spin density distribution at 0.002 density contour; whereas Figure 3C shows the edge view for the 0.02 contour which emphasizes those regions of higher spin density. The spin is largely in a π-p orbital on C-12.

Our findings complement and help to explain experimental work mentioned in the Introduction which showed that for DNA−acrylamide at 77 K the spin density is mainly on the DNA bases cytosine and thymine, but after annealing to 130 K, which we presume activates the proton transfer, the spin density shifts to the acrylamide portion of the complex with the rapid formation of radical **III**. The experimentally observed process is relatively complex as the excess electrons in irradiated hydrated DNA at 77 K reside on both cytosine and thymine

with greater amounts usually on cytosine.[12a,19,20] For DNA annealing to 130 K activates the electron transfer from thymine to cytosine.[19c] However, electrons trapped initially on cytosine are stabilized by a proton transfer from its complementary base, guanine, and electron transfer processes from electrons on cytosine are not thermally activated until higher temperatures are reached−greater than 150 K.[19c] Thus the results observed by electron spin resonance (ESR) with DNA show a DNA doublet spectrum from both cytosine and thymine.[12a,19,20] On DNA complexation with acrylamide, DFT theory predicts that the thymine−acrylamide complex would share the unpaired electron and the large doublet might be predicted to be lost in the DNA ESR spectrum. However, experimental work shows the ESR doublet spectrum is still present and this is expected since cytosine electron adduct radicals and uncomplexed thymine anion radicals are still present. Experiment shows that on annealing the DNA complex to 130 K radical **III** is produced, presumably by PA-ET (reaction A) followed by rearrangement (reaction B). Further annealing beyond 150 K produces additional amounts of radical **III** by activation of the electron transfer from cytosine electron adduct radicals through DNA presumably via a hopping/tunneling mechanism to thymine−acrylamide complexes.[19c,d]

A possible confusion about the mechanism under investigation is whether reaction A (Figure 1) is a proton-assisted electron transfer or a simple hydrogen atom shift from thymine to the acrylamide. While this can be incorrectly viewed as semantics it is an important distinction. A proton-assisted excess electron transfer is a process in which a proton shifts position and concertedly drives a spatially separated excess electron from one structure to another. For an excess electron transfer process such as in this work, there should be no significant unpaired spin on the proton during the process. A hydrogen atom shift would occur when the electron and proton shift as a neutral unit with the electron localized near the proton during the process; otherwise, if electron and proton are not spatially proximate, then it is a simultaneous proton and electron transfer. The spin distributions shown in Figure 2 and tabulated in Table 3 indicate that the electron spin density resides in the delocalized π-systems of the thymine and acrylamide molecules before and after the proton transfer with no significant spin at the proton before or after the transfer. This is not surprising since the electron is in the π-system and the proton in the σ-system. At intermediate proton-transfer distances one might argue that spin might localize on the transferring proton. To test this we performed two single-point DFT calculations with the transferring proton at intermediate distances (1.42−1.46 Å bond distances) with the remaining geometry as in structure **I** or in structure **II**. Both of these calculations show no significant electron spin on the transferring proton at these halfway points. There can be no other conclusion than that reaction A (Figure 1) is predicted by theory to be a PA-ET reaction and not a hydrogen atom shift.

Conclusions

Our theoretical results at the density function theory levels predict that the proton-assisted electron transfer is favorable after electron attachment to an isolated thymine−acrylamide complex. The ca. 2 kcal/mol free energy change for the PA-ET suggests an equilibrium process between species **I** and **II** that is then driven to the final product (**III**) by an irreversible intramolecular rearrangement reaction in species **II**. These results are in accord with our previous experimental results[15] and serve as an example of the potential for electron affinic agents that hydrogen bond to DNA to undergo PA-ET and thus act as irreversible electron sinks.[15] Such species would sensitize DNA to radiation damage as they would prevent recombination of the electron and hole, which is a protective event, and additionally may form new reactive intermediates that are themselves damaging.[12]

Acknowledgment. This research was supported by the NIH-NCI Grant RO1 CA45424 and by the Oakland University Research Excellence Fund.

References and Notes

(1) (a) Mitchell, P. *Nature* **1961**, *191*, 144. (b) Mitchell, P. *Science* **1979**, *206*, 1148.

(2) Onsager, L. *Science* **1967**, *156*, 541; **1969**, *166*, 1359.

(3) Kohen, A.; Klinman, J. P. *Acc. Chem. Res.* **1998**, *31*, 397; *Chem. Biol*. **1999**, *6*, R191.

(4) Meyer, T J. *J. Electrochem. Soc*. **1984**, *131*, 221C.

(5) Pecoraro, V. L.; Baldwin, M. J.; Caudle, M. T.; Hsieh, W. Y.; Law, N. A. *Pure Appl. Chem*. **1998**, *70*, 925.

(6) Babcock, G. T.; Barry, B. A.; Debus, R. J.; Hoganson, C. W.; Atamian, M.; McIntosh, L.; Sithole, I.; Yocum, C. F. *Biochemistry* **1989**, *28*, 9557.

(7) Paddock, M. L.; McPherson, P. H.; Feher, G.; Okamura, M. Y. *Proc. Natl. Acad. Sci. U.S.A.* **1990**, *87*, 6803.

(8) Malstrom, B. G. *Chem. Rev*. **1990**, *90*, 1247; *Acc. Chem. Res.* **1993**, *26*, 332.

(9) Chan, S. I.; Li, P. M. *Biochemistry* **1990**, *29*, 1.

(10) (a) Cukier, R. I. *J. Phys. Chem.* **1994**, *98*, 2378; **1995**, *99*, 16101; **1996**, *100*, 15428; **1999**, *103*, 5989. (b) Cukier, R. I.; Nocera, D. G. *Annu. Rev. Phys. Chem.* **1998**, *49*, 337.

(11) Bernhard, W. A.; Milano, M. T. *Radiat. Res.* **1999**, *151*, 39−49.

(12) (a) Becker, D.; Sevilla, M. D. The Chemical Consequences of Radiation Damage to DNA. In *Advances in Radiation Biology*; Lett, J., Ed.; Academic Press: New York, 1993; Vol. 17, pp 12, 1−180. (b) Sevilla, M. D.; Becker, D.; Razskazovskii, Y. *Nukleonika* **1997**, *42*, 283−92. (c) Colson, A. O.; Sevilla, M. D. *Int. J. Radiat. Biol.* **1995**, *67*, 627−45. (d) Colson, A. O.; Besler, B.; Sevilla, M. D. *J. Phys. Chem.* **1992**, *96*, 9788−9794.

(13) Dixon, D. W.; Thornton, N. B.; Netzel, T. *Inorg. Chem.* **1999**, *38*, 5526.

(14) Shafirovich, V.; Dourandin, A.; Luneva, N. P.; Geacintov, N. E. *J. Phys. Chem. B* **2000**, *104*, 137

(15) Razskazovskii, Y.; Roginskaya, M,; Sevilla, M. D. *Radiat. Res.* **1998**, *149*, 422.

(16) Van Paemel, C.; Frumin, H.; Brooks, V. L.; Failor, R.; Sevilla, M. D. *J. Phys. Chem.* **1975**, *79*, 839.

(17) Wilson, W. D. *Nucleic Acids in Chemistry and Biology*; Oxford University Press: New York, Tokyo, 1996; Chapter 8.

(18) (a) Razskazovskii, Y.; Swarts, S. G.; Falcone, J. M.; Taylor, C.; Sevilla, M. D. *J. Phys. Chem. B* **1997**, *101*, 1460−7. (b) Wang, W.; Sevilla, M. D. *Radiat. Res*. **1994**, *138*, 9−17.

(19) (a) Yan, M.; Becker, D.; Summerfield, S.; Renke, P.; Sevilla, M. D. *J. Phys. Chem*. **1992**, *96*, 1983. (b) Messer, A.; Carpenter, K.; Forzley, K.; Buchanan, J.; Yang, S.; Razskazovkii, Y.; Cai, Z.; Sevilla, M. D. *J. Phys. Chem. B* **2000**, *104*, 1128−36. (c) Wang, W.; Sevilla, M. D. *Radiat. Res.* **1994**, *138*, 9−17. (d) Cai, Z.; Gu, Z.; Sevilla, M. D. *J. Phys. Chem. B* **2000**, *104*, 10406−11.

(20) Wang, W.; Yan, M.; Becker, D.; Sevilla, M. D. *Radiat. Res*. **1994**, *137*, 2

(21) Peluso, A.; Brahimi, M.; Del Re, G. *J. Phys. Chem. A* **1998**, *102*, 10333; *Chem. Phys. Lett.* **1999**, *299*, 511

(22) Di Donato, M.; Borelli, R.; Capobianco, A.; Monaco, G.; Improta, R.; Brahimi, M.; Peluso, A. *Adv. Quantum Chem.* **1999**, *36*, 301

(23) Galbraith, J. M.; Schaefer, H. F., III. *J. Chem. Phys.* **1996**, *105*, 862

(24) Roesch, N.; Trickey, S. B. *J. Chem. Phys.* **1997**, *106*, 8940.

(25) Frisch, M. J.; Trucks, G. W.; Schlegel, H. B.; Scuseria, G. E.; Robb, M. A.; Cheeseman, J. R.; Zakrzewaki, J. R.; Montgomery, J. A.; Stratmann, R. E.; Burant, J. C.; Dapprich, S.; Millam, J. M.; Daniels, A. D.; Kudin, K. N.; Strain, M. C.; Farkas, O.; Tomasi, J.; Barone, V.; Cossi, M.; Cammi, R.; Mennucci, B.; Pomelli, C.; Adamo, C.; Clifford, S.; Ochterski, J.; Petersson, G. A.; Ayala, P. Y.; Cui, Q.; Morokuma, K.; Malick, D. K.; Rabuck, A. D.; Raghavachari, K.; Foresman, J. B.; Cioslowski, J.; Ortiz, J. V.; Stefanov, B. B.; Liu, G.; Liashenko, A.; Piskorz, P.; Komaromi, I.; Gomperts, R.; Martin, R. L.; Fox, D. J.; Keith, T.; Al-Laham, M. A.; Peng, C. Y.; Nanayakkara, A.; Gonzalez, C.; Challacombe, M.; Gill, B. G.; Hohnson, P. M. W.; Chen, W.; Wong, M. W.; Andrew, J. L.; Head-Gordon, M.; Replogle, E. S.; Pople, J. A. *Gaussian 98*, revision A.7; Gaussian, Inc.: Pittsburgh, PA, 1998.